



Article Processing Dates: Received on 2023-08-11, Reviewed on 2023-09-07, Revised on 2023-09-24, Accepted on 2024-03-29 and Available online on 2024-04-30

## Design and simulation of offshore crane structure with capacity of 400 ton

Freddy Marpaung<sup>1\*</sup>, Harry Purnama<sup>1</sup>, I Nyoman Artana<sup>2</sup>, Nani Kurniawati<sup>2</sup>, Dian Samodrawati<sup>3</sup>, Tri Surawan<sup>2</sup>, Harini Agusta<sup>4</sup>

<sup>1</sup>Research Center of Process and Manufacture Technology Industry, National Research and Innovation Agency, South Tangerang, 15314, Indonesia

<sup>2</sup>Mechanical Engineering, Universitas Jayabaya, East Jakarta, 16452, Indonesia

<sup>3</sup>Electrical Engineering, Universitas Jayabaya, East Jakarta, 16452, Indonesia

<sup>4</sup>Chemical Engineering, Universitas Jayabaya, East Jakarta, 16452, Indonesia

\*Corresponding author: fred003@brin.go.id

### Abstract

Offshore cranes are transport machines which are used to lift a heavy load to other places. The weight and strength of a crane are crucial parameters that must be considered during the design stage. There are many ways to optimize these aspects, such as suitable material selection and virtual simulation assistance using ANSYS software. The main goal of this study is to design and develop a structurally stable crane on the ship deck. This crane is modeled using CATIA software and analyzed using ANSYS software to obtain stress and displacement distribution on the crane structure. Maximum load is applied for four different elevation angles, namely (30°, 43°, 60°, and 80°). From the static structural simulation, the highest stress is obtained when the elevation angle of 30° is about 1030 MPa and deformation is 461.24 mm. The minimum fatigue life of the offshore crane at a luffing angle of 43° is 659.14 cycles.

### Keywords:

Offshore crane, structure analysis, stress, fatigue, CAE.

### 1 Introduction

Indonesia is an archipelagic country with relatively high water traffic due to the increasing volume of loading and unloading of imported goods and inter-insular trade [1]. To support the process of distributing export and import goods, it is necessary to improve the maritime transportation system by replacing an obsolete offshore platform. Dead Weight Load (DWT) container ships are a type of container transport ship that uses cranes for loading and unloading equipment. An offshore crane is loading and unloading equipment specifically designed for a ship deck. Cranes work by lifting the material, moving it horizontally, and then lowering the material to the desired place [2]. This machine has a large shape and carrying capacity and it is able to rotate the loads 360 degrees with a range of up to tens of meters. Offshore cranes generally consist of a crane mast, boom, crane housing, cargo block, sling, and motor [3].

To support the process of loading and unloading containers smoothly, the reliability of the crane used is important. The strength and weight of the crane are important factors at the crane design stage. The design stage is crucial because it determines the

characteristics of the crane structure. Based on this, inappropriate decisions at this stage must be minimized because they may cause expensive consequences in the subsequent development process. The design stage of the crane structure commences with creating a 3D CAD model. Based on the 3D CAD model, the strength of the crane structure is investigated when the maximum load is applied. Then, the test results from the 3D technical drawings are evaluated and updated to obtain an appropriate design structure [4]. After that, the latest updated prototype is produced and the cycle of stages continues until it meets safety standards. Such conventional processes are time-consuming and require high costs.

These shortcomings can be eliminated by using virtual models as an alternative to conventional testing and prototyping updating processes. Dewi *et al.* compared the results of pedestal crane structural tests using ANSYS with hand calculations. They used static simulation test results as load-based in dynamic testing to determine the critical point and fatigue life of the crane structure. The results of their research show that operational loads have the largest contribution (80.7%) to fatigue life, followed by wind loads (19.3%) and wave loads (0%), and the design life is 96.5 years or around 5x that of design life [5]. Seong *et al.* [6] carried out statistic structural tests and CFX analysis at different luffing angles. Urbaš *et al.* developed a mathematical model to analyze the dynamics of boom cranes by taking into account the influence of load geometry, sling rope system, and drive and link flexibility. The model was validated using the commercial programs MSC.Adams and ANSYS-MSC.Adams and the result reveal that representing the load as a lumped mass, a typical simplification in literature, versus modeling it as a rigid body with specific geometry significantly affects the predicted dynamics of the crane-load system, markedly impacting the load's kinetic energy [7]. Shangbin *et al.* employs a finite element analysis (FEA) methodology to assess the mechanical properties of a crane boom head model. The objective is to optimize the boom head design to enhance its reliability and stress limitations during the operating process. The findings indicate that the optimized model exhibits superior mechanical performance, suggesting that it is a more suitable solution for practical applications [8]. Han *et al.* reported an analysis of an offshore crane platform, aiming to investigate deformation and stress distribution, in addition, they made precise estimates to determine the life cycle of the welded boom structure. The analysis carried out includes the crane's own weight, maximum working load, wind pressure and waves that cause the ship to roll [9]. Iwona *et al.* developed a spatial model of a crane with flexible booms, cylinders, and a rope system, validated through both numerical simulations and experiments. The model is capable of efficient testing of different configurations and load conditions during the design stage, providing valuable information for the selection of appropriate materials, structural dimensioning, and the approval of regulatory standards [10].

Jinpeng *et al.* studied on the dynamic characteristics of a tower crane with an anti-back-tipping device is conducted to address the back-tipping failure risk during sudden unloading. Modal analysis, considering Rayleigh damping and nonlinear dynamics, is performed using finite element methods to assess the crane's components and prevent potential failures, focusing on load distribution plate pressure variations during sudden unloading for practical engineering guidance [11]. Ozgucet *et al.* successfully conducted non-linear finite element of ship-shaped offshore vessels, in which the deck frame is exposed to buckling failure. A hybrid approach (combination of the deformable finite elements and the concentrated mass method) was applied into model of some offshore structures [12]. Another group also reported simulation of crane structure using ABAQUS and fe-safe to measure strength and fatigue life of the crane structure [13], [14].

This study aims to identify the distribution of stress and deformation in the crane structure so that critical areas can be identified when the crane is loaded with a maximum load (400

tons) at several different elevation angles. In addition, this study was performed to gain information on crane operating parameters and acquire the best crane design in terms of construction.

## 2 Research Methodology

### 2.1 Method

The methodology used in this research includes modeling of an offshore crane using CATIA software. Furthermore, static structural analysis was carried out using finite element software (ANSYS). The main parameters are set to assess the mechanical performance of crane components at different elevation angles. The load distribution and reactions of all components are displayed when simulated with ANSYS software (Fig. 1).

#### 2.1.1 Static Structural Analysis

Finite element analysis is used to investigate critical areas of the crane structure. The crane was designed using CATIA software, then CAD was imported into ANSYS Design Modeler. The CAD modeling results are shown in Fig. 2. The mathematical formula used in static structural stress simulations shown in Eq. 1 – Eq. 3 [15].

$$\frac{\partial \sigma_{xx}}{\partial x} + \frac{\partial \sigma_{xy}}{\partial y} + \frac{\partial \sigma_{xz}}{\partial z} + b_x = 0, \quad (1)$$

$$\frac{\partial \sigma_{yx}}{\partial x} + \frac{\partial \sigma_{yy}}{\partial y} + \frac{\partial \sigma_{yz}}{\partial z} + b_y = 0, \quad (2)$$

$$\frac{\partial \sigma_{zx}}{\partial x} + \frac{\partial \sigma_{zy}}{\partial y} + \frac{\partial \sigma_{zz}}{\partial z} + b_z = 0, \quad (3)$$

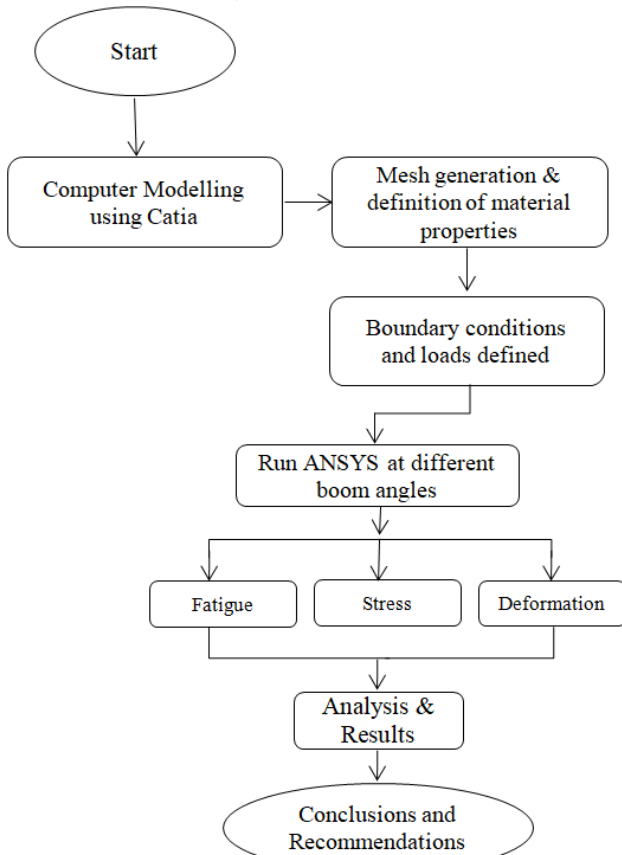


Fig. 1. Research methodology flowchart.

Material deformation is determined using displacement and strain. The displacement gradient in three coordinate systems, as shown in Eq. 4 – Eq. 5, expresses the rate of change of displacement at a specific point in the material.

$$\varepsilon_{xx} = \frac{\partial u_x}{\partial x}, \varepsilon_{yy} = \frac{\partial u_y}{\partial y}, \varepsilon_{zz} = \frac{\partial u_z}{\partial z} \quad (4)$$

$$\varepsilon_{xy} = \frac{1}{2} \left[ \frac{\partial u_x}{\partial y} + \frac{\partial u_y}{\partial x} \right], \varepsilon_{xz} = \frac{1}{2} \left[ \frac{\partial u_x}{\partial z} + \frac{\partial u_z}{\partial x} \right], \varepsilon_{yz} = \frac{1}{2} \left[ \frac{\partial u_y}{\partial z} + \frac{\partial u_z}{\partial y} \right] \quad (5)$$

The superposition procedure is used to combine and generalize stress components under different loading conditions. The relationship between force and the strain caused by that force is given by Hooke's law. To improve the accuracy of this method, the resulting stress must have a linear relationship to the load and there will be small-scale deformations in the given model compared to the structure as a whole. Therefore, Eq. 6 – Eq. 8 is used to describe multiaxial loading of homogeneous isotropic materials.

$$\varepsilon_x = \frac{1}{E} \left[ \sigma_x - \nu \sigma_y - \nu \sigma_z \right] \quad (6)$$

$$\varepsilon_y = \frac{1}{E} \left[ -\nu \sigma_x + \sigma_y - \nu \sigma_z \right] \quad (7)$$

$$\varepsilon_z = \frac{1}{E} \left[ -\nu \sigma_x - \nu \sigma_y + \sigma_z \right] \quad (8)$$

#### 2.1.2 Boundary Conditions

Boundary conditions in static structural analysis are shown in Fig. 3. In this study, a load of 400 tons was given at 4 different luffing angles, namely (30°, 48°, 60° and 80°). The combination of different luffing angles at maximum load is carried out to obtain safe operating conditions when the crane is given maximum load and simplify the investigation of stress and displacement distribution in the crane structure.

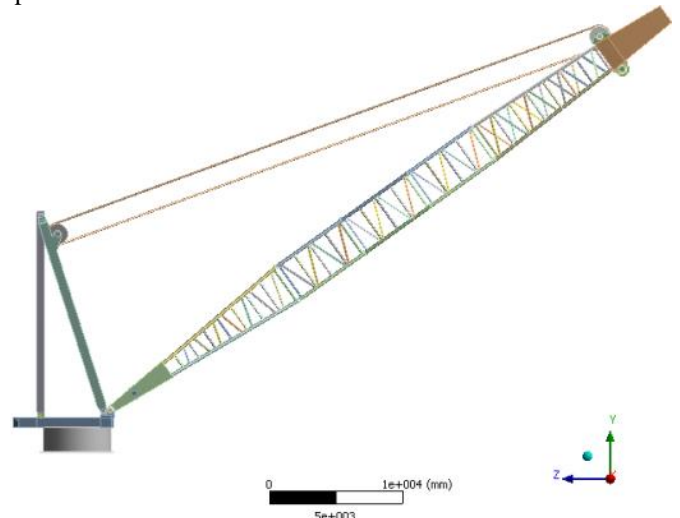


Fig. 2. Cad model of crane structure.

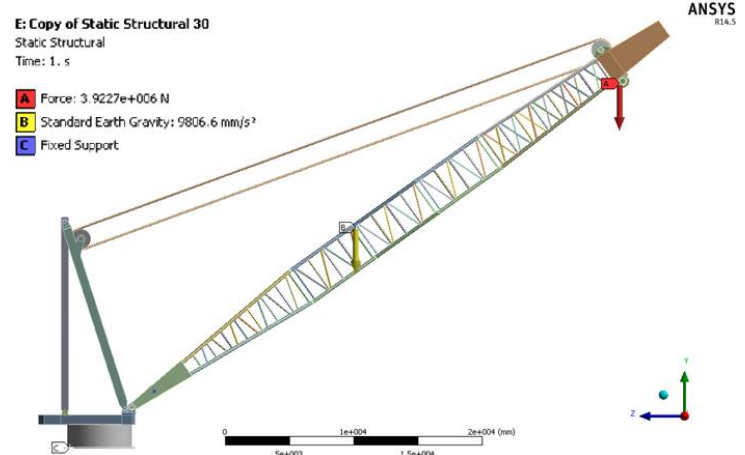


Fig. 3. Boundary conditions.

### 2.1.3 Mesh Generation

Meshing is a technique for partitioning a model into several elements. All parts of the offshore crane structure are modeled with a dominant tetrahedron. In Fig.4, it can be seen that meshing produces 5492345 nodes and 2811359 elements. To ensure that the mesh has been carried out properly, the mesh metric check is carried out with an average orthogonal quality criterion of 0.799, where this result is sufficient to support the static analysis carried out [2], [3].

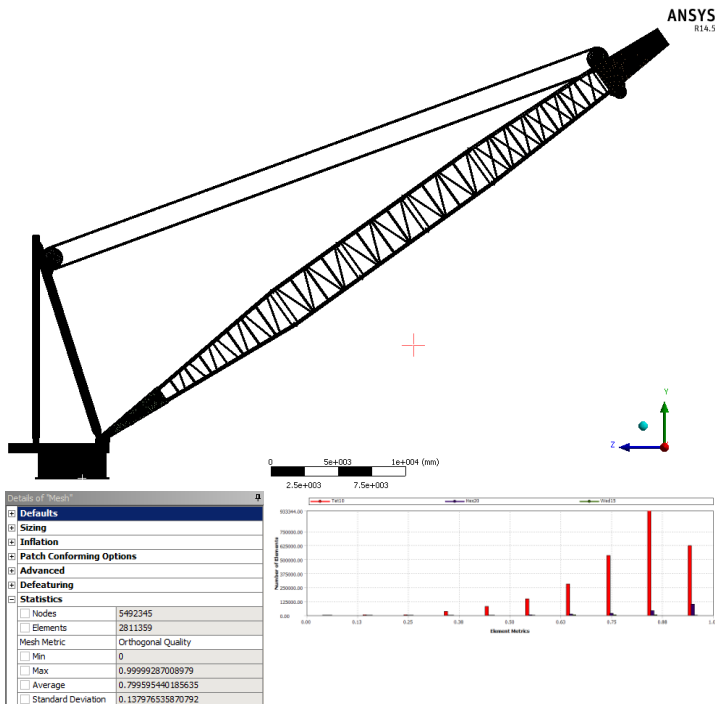


Fig. 4.3D model of the crane structure and its mesh model in ANSYS Workbench R14.5.

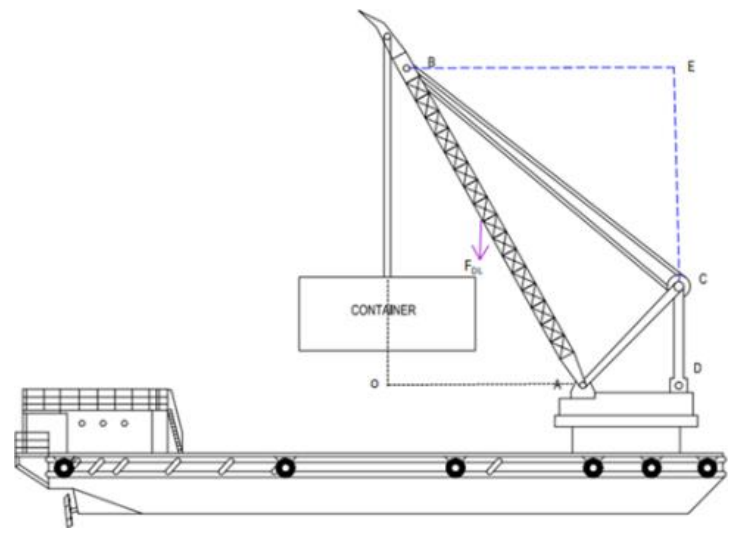
### 2.2 Material

TS 890 is a structural steel used for the finite element method simulations of crane structures. This material is a high-strength steel alloy with a heat treatment process (quenching and tempering). This material has a minimum yield strength of 890 MPa and a maximum tensile strength of 1040 MPa.

## 3 Results and Discussion

### 3.1 Hand Calculation

Manual calculation of the forces acting on the crane structure is shown in Fig. 5. From the results of the calculations, it was obtained that the highest force was at the support points C and D, namely 57583.75 kN. This is matched by a previous virtual test, where the maximum stress occurs in this area.



Dead load	: 268.16	ton
Dead load, DL (ton/m)	: 47.83	kN/m
Lifted load, LL	: 3927	kN
Length of AB	: 55	m
Length of AD	: 5	m
Length of CD	: 15	m
Length of AC	: 15.81	m
Length of AO	: 40.22	m
Distance of B to the load	: 3	m
Length of OB	: 37.51	m
Length of CE	: 22.51	m
Length of AP	: 20.11	m
Angle of $\Delta_{ACD}$	: 18.43	°
Triangle $\Delta_{CAD}$	: 71.57	°
Triangle $\Delta_{OAB}$	: 43	°

$$\Sigma M_A = 0 \rightarrow F_D \times AD + F_{DL} \times DL - LL \times AO = 0$$

$$\rightarrow F_D = 57583,75 \text{ kN (tarik)}$$

$$F_C = -57583,75 \text{ kN (tekan)}$$

$$F_A = -52061,66 \text{ kN (tekan)}$$

$$F_{CB} = 18389,95 \text{ kN (tarik)}$$

Fig. 5. Schematic of free-body diagram of crane used to calculate the force components.

### 3.2 Static Structural Simulation

At the design stage of the offshore crane, it is necessary to perform load simulations to obtain information regarding safe working loads when the crane is operated in a platform deck. The static loading analysis of the crane presented in this article focuses on the strength of the crane structure when receiving maximum load at several different elevation angles. In this simulation, the crane was loaded with the weight from slings, lifting load of 400 tons, and weight from the crane structure. The analysis results show that the maximum stress occurred in the pedestal area which was in contact with the pin from the bottom of the frame as shown in Fig. 6. This occurs due to the boom hanging in the direction of gravity. Meanwhile, the maximum deflection occurred at the end of the boom.

Simulation results at a boom angle of 30° show that the crane structure was expected to experience plastic damage because the stress value exceeded the yield strength (890 MPa). The maximum stress at an angle of 30° was 1078.6 MPa with a maximum deformation of 482.96 mm.

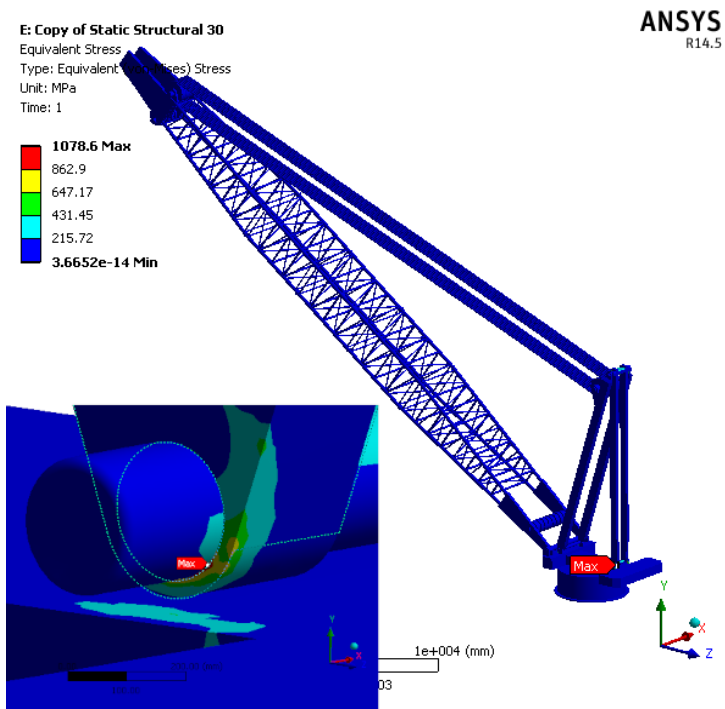


Fig. 6. Location of maximum Von Mises stress.

In addition, the deformation and stress distribution of the boom has some changes in ANSYS value at different angles of elevation; with the increase of the elevation of the boom, the maximum value of the stress of the boom gradually moves to the root of the boom.

As shown in Table 1, when the range of the elevation of the boom is 30°-80°, the stress and deformation of the boom decreases with the increased of the elevation.

Boom angle	Von Misses Stress	Total Deformation
30	1030.1 MPa	461.24 mm
43	838.2 MPa	393.00 mm
60	608.32 MPa	333.03 mm
80	493.3 MPa	233.13 mm

The results show that Von Mises stress of the boom at three different lift angles (43°-80°) is still below the yield strength of the material. This indicates that the design of the offshore crane is workable as it can endure the amount of stress that is stated in Table 2.

Table 2. Mechanical properties of TS 890

Grade	WT (mm)	Minimum Yield Strength (MPa)				Tensile Strength (MPa)			Min. Elong. Long%	Min. Elong. Transv%
		≤ 12	> 12 ≤ 20	> 20 ≤ 40	> 40 ≤ 50	≤ 20	> 20 ≤ 40	> 40 ≤ 50	All	All
TS 890		890	850	820	960-1130	920-1090	870-1040	14	12	

Fig. 7 is a visualization of the stress distribution on the boom of an offshore crane, where the highest stress is 321.04 MPa, located at the bottom of the boom. Meanwhile, the stress on other parts of the boom is still below 100 MPa or below 10% of the equivalent stress of the crane material. The fatigue results for the crane structure were carried out at an angle of 43°, this is because the maximum stress that occurs in the crane structure is still below the yield strength of the material, the minimum value of the fatigue results is 659.14 cycles. Detailed images can be seen in Fig.8.

Fig. 7. Stress distribution on the crane with boom angle 43°.

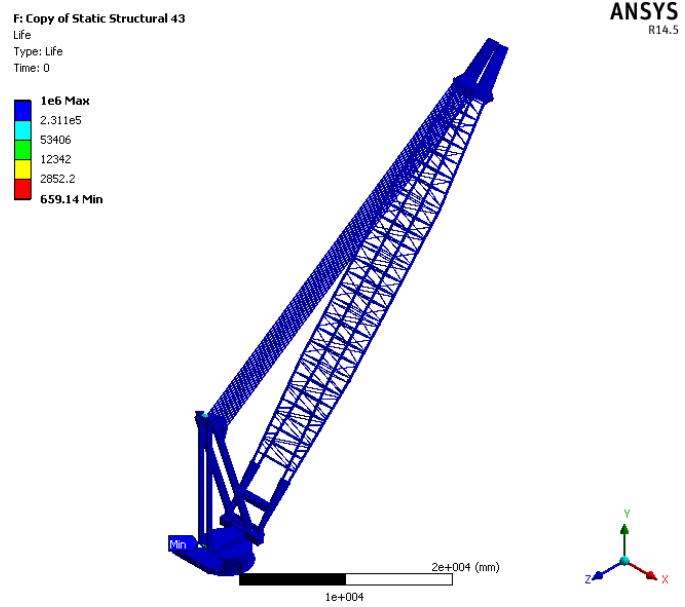
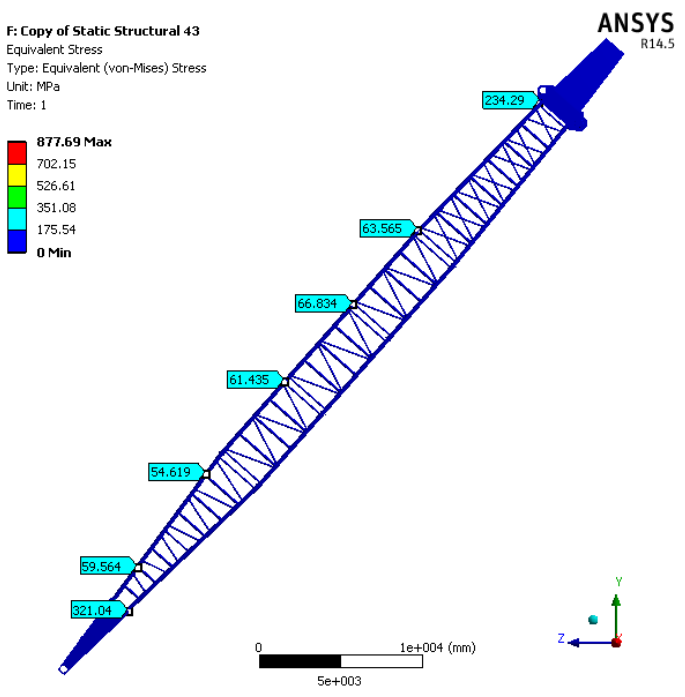


Fig. 8. Fatigue on the crane with boom angle 43°.



#### 4 Conclusion

Modeling using finite element software can simplify the process of calculating the strength of crane structures and predicting failures that will occur in parts of the crane structure. Numerical simulation results show that operating the crane at an elevation angle of 30° has the potential to cause material failure because the von Misses stress value that occurs exceeds the yield strength of the material, while the maximum load at other elevation angles is still in the safe category. The fatigue strength at

an angle of 43° is used to calculate the life cycle of the crane model, wherein the life cycle is obtained at 659.14 cycles.

## References

- [1] A. Ardiansyah, “Pelaksanaan Bongkar Material Kontruksi PT. Semen Imasco Asiatic Puger Pada Kapal MV. Sun Unity Oleh Badan Usaha Pelabuhan PT. Delta Artha Bahari Nusantara Cabang Probolinggo di Pelabuhan Probolinggo,” Semarang, 2021. [Online]. Available: <http://repository.unimar-amni.ac.id/3952/>
- [2] B. Noori Khudhur, “Finite Element Analysis of the Boom of Crane Loaded Statically,” *Eng. Technol. J.*, vol. 31, no. 9, pp. 1626–1639, 2013, doi: 10.30684/etj.2013.82179.
- [3] S. Wang, Z. Ren, G. Jin, and H. Chen, “Modeling and Analysis of Offshore Crane Retrofitted with Cable-Driven Inverted Tetrahedron Mechanism,” *IEEE Access*, vol. 9, pp. 86132–86143, 2021, doi: 10.1109/ACCESS.2021.3063792.
- [4] K. Abdullah, S. Sumardiono, and H. Soeroso, “Strength Analysis of the Deck Crane Barge Using the Finite Element Method,” in *Proceedings of the 1st International Conference on Sustainable Engineering Development and Technological Innovation, ICSEDTI 2022, 11-13 October 2022, Tanjungpinang, Indonesia*, 2023. doi: 10.4108/eai.11-10-2022.2326425.
- [5] D. A. Dewi and J. B. Ariatedja, “Fatigue Analysis of Pedestal-mounted Crane on Offshore Fixed Platform Using Finite Element Method,” *Int. J. Mech. Eng. Sci.*, vol. 3, no. 2, p. 38, 2019, doi: 10.12962/j25807471.v3i2.9387.
- [6] H.-J. Seong, C.-K. Jeong, J.-H. Jeon, S.-H. Park, Y.-G. Jung, and S.-C. Huh, “A Safety Evaluation of Offshore Lattice Boom Crane,” in *Proceedings of the 2018 International Conference on Computer Modeling, Simulation and Algorithm (CMSA 2018)*, Atlantis Press, 2018, pp. 275–280. doi: 10.2991/cmsa-18.2018.62.
- [7] A. Urbaś, K. Augustynek, and J. Stadnicki, “Dynamics analysis of a crane with consideration of a load geometry and a rope sling system,” *J. Sound Vib.*, vol. 572, p. 118133, 2024, doi: <https://doi.org/10.1016/j.jsv.2023.118133>.
- [8] S. Yang, J. Yang, and J. Cai, “Reliability-based topology optimization of large-tonnage crane boom head with stress constraint,” *Proc. Inst. Mech. Eng. Part C J. Mech. Eng. Sci.*, p. 09544062241228983, Feb. 2024, doi: 10.1177/09544062241228983.
- [9] D. S. Han, S. W. Yoo, H. S. Yoon, M. H. Kim, S. H. Kim, and J. M. Lee, “Coupling analysis of finite element and finite volume method for the design and construction of FPSO crane,” *Autom. Constr.*, vol. 20, no. 4, pp. 368–379, 2011, doi: 10.1016/j.autcon.2010.11.007.
- [10] I. Adamiec-Wójcik, Ł. Draj, M. Metelski, K. Nadratowski, and S. Wojciech, “A 3D model for static and dynamic analysis of an offshore knuckle boom crane,” *Appl. Math. Model.*, vol. 66, pp. 256–274, 2019, doi: <https://doi.org/10.1016/j.apm.2018.09.006>.
- [11] J. Gu, Y. Qin, Y. Xia, J. Wang, H. Gao, and Q. Jiao, “Failure Analysis and Prevention for Tower Crane as Sudden Unloading,” *J. Fail. Anal. Prev.*, vol. 21, no. 5, pp. 1590–1595, 2021, doi: 10.1007/s11668-021-01201-y.
- [12] O. Ozguc, “Assessment of buckling behaviour on an fpso deck panel,” *Polish Marit. Res.*, vol. 27, no. 3, pp. 50–58, 2020, doi: 10.2478/pomr-2020-0046.
- [13] R. Buczkowski and B. Żyliński, “Finite element fatigue analysis of unsupported crane,” *Polish Marit. Res.*, vol. 28, no. 1, pp. 127–135, 2021, doi: 10.2478/pomr-2021-0012.
- [14] W. Zhu, Y. Li, Y. Jiang, Y. Deng, and Y. Dong, “Load-spectrum-based high-cycle fatigue life assessment of the crane arms,” in *Proc.SPIE*, Apr. 2024, p. 130821Z. doi: 10.1117/12.3026392.
- [15] S. Echaroj, N. Pannucharoenwong, and P. Rattanadecho, “Development of vehicle chassis from novel materials for light weight electric shuttles using finite element analysis,” *Sci. Technol. Asia*, vol. 26, no. 3, pp. 64–76, 2021.